JOURNAL OF VIROLOGY, Sept. 1994, p. 5568–5578
0022-538X/94/$04.00+0

Vol. 68, No. 9

Large Deletion Mutations Involving the First Pyrimidine-Rich Tract of the 5′ Nontranslated RNA of Human Hepatitis A Virus Define Two Adjacent Domains Associated with Distinct Replication Phenotypes

DAVID R. SHAFFER,[1] EDWIN A. BROWN,[2]† AND STANLEY M. LEMON[1,2]*

Departments of Microbiology and Immunology[1] and Medicine,[2] The University of North Carolina at Chapel Hill, Chapel Hill, North Carolina 27599-7030

Received 5 May 1994/Accepted 9 June 1994

The 5′ nontranslated RNA (5′NTR) of the HM175 strain of human hepatitis A virus contains several pyrimidine-rich regions, the largest and most 5′ of which (pY1) is an almost pure polypyrimidine tract located between nucleotides (nt) 99 and 138, which includes five tandem repeats of the sequence motif (U)UUCC(C). Previous modeling of the RNA secondary structure suggested that this region was likely to be single-stranded, but repetitive RNase V1 cleavage sites within these (U)UUCC(C) motifs indicated that pY1 possesses an ordered structure. To assess the role of this domain in replication of the virus, a series of large deletion mutations were created which involved the pY1 domain of an infectious cDNA clone. Deletion of 44 nt between nt 96 and 139, including the entire pY1 domain, did not reduce the capacity of the virus to replicate in BS-C-1 or FRhK-4 cells, as assessed by the size of replication foci in radioimmunofocus assays or by virus yields under one-step growth conditions. In contrast, viable virus could not be recovered from transfected RNAs in which the deletion was extended in a 5′ direction by an additional 3 nt (Δ93-134), most likely because of the destabilization of a predicted stem-loop structure upstream of pY1. Deletion mutations extending in a 3′ fashion to nt 140, 141, or 144 resulted in moderately (Δ96-140 and Δ96-141) or strongly (Δ99-144, Δ116-144, and Δ131-144) temperature-sensitive replication phenotypes. Although deletion of the pY1 domain did not by itself affect the replication phenotype of virus, the additional deletion of sequence elements within the pY1 domain (nt 99 to 130) substantially enhanced the temperature-sensitive phenotype of Δ131-144 virus. These data suggest that the (U)UUCC(C) motifs within the pY1 domain are conserved among wild-type viruses in order to serve a function required during infection in vivo but not in cell culture. In contrast, the single-stranded region located immediately downstream of pY1 (nt 140 to 144) is essential for efficient replication in cultured cells at physiological temperature. Viruses with deletion mutations involving nt 140 to 144 and viruses with large pY1 deletions but normal replication phenotypes in cell culture may have attenuation properties which could be exploited for vaccine development.

Like other members of the picornavirus family, hepatitis A virus (HAV [genus *Hepatovirus*]) contains a single-stranded, positive-sense RNA genome with a lengthy (735 nucleotides [nt]) 5′ nontranslated region (5′NTR). The 5′NTR of HAV (HM175 strain) contains an internal ribosomal entry site (IRES) located between nt 152 and nt 735, which regulates cap-independent, internal initiation of translation of the viral polyprotein, although the level of efficiency with which the HAV IRES promotes translation is much lower than that of other picornavirus IRES elements both in vivo and in vitro (4, 27). In addition, the 5′NTR of HAV is likely to have other functions which are essential for virus replication, including control of positive-strand RNA synthesis and possibly encapsidation (1).

Although there are substantial differences between the predicted secondary structures of the 5′NTRs of HAV and those of all other picornaviruses, the secondary structure of the HAV 5′NTR more closely resembles that of the cardioviruses and aphthoviruses than the corresponding structure in rhinoviruses and most enteroviruses (3). Among other similarities, the 5′NTRs of hepatoviruses, cardioviruses, and aphthoviruses share the potential to form two or more pseudoknots in the noncoding region upstream of the IRES element (3, 4, 6, 16, 19, 25). Also present in this region is a pyrimidine-rich sequence which consists of an almost pure poly(C) tract in the cardioviruses and aphthoviruses. In the hepatoviruses, the corresponding region contains a mixture of uridylic acids and cytidylic acids (in a 24:14 ratio in the HM175 strain of HAV), with only two purines located within a 40-nt-long, nearly pure polypyrimidine tract (pY1 domain [nt 99 to 138]) (Fig. 1). In each of these virus genera, this pyrimidine-rich tract appears to separate two discrete regions of RNA secondary structure (3, 6). A similarly located pyrimidine-rich tract is not found in either the enterovirus or rhinovirus 5′NTR.

There are other pyrimidine-rich tracts within the 5′NTR of HAV (5), but the pY1 domain is the lengthiest and most prominent of these regions. Although considerable sequence heterogeneity exists within this domain among different human hepatoviruses (Fig. 2) (3), the general features of this domain are conserved among all strains of HAV. A striking aspect of the pY1 domain, which is unique to the HAV 5′NTR among all other picornaviral 5′NTRs, is the presence of tandem

* Corresponding author. Phone: (919) 966-2536. Fax: (919) 966-6714.

† Present address: Infectious Disease Division, Medical University of South Carolina, Charleston, SC 29425.

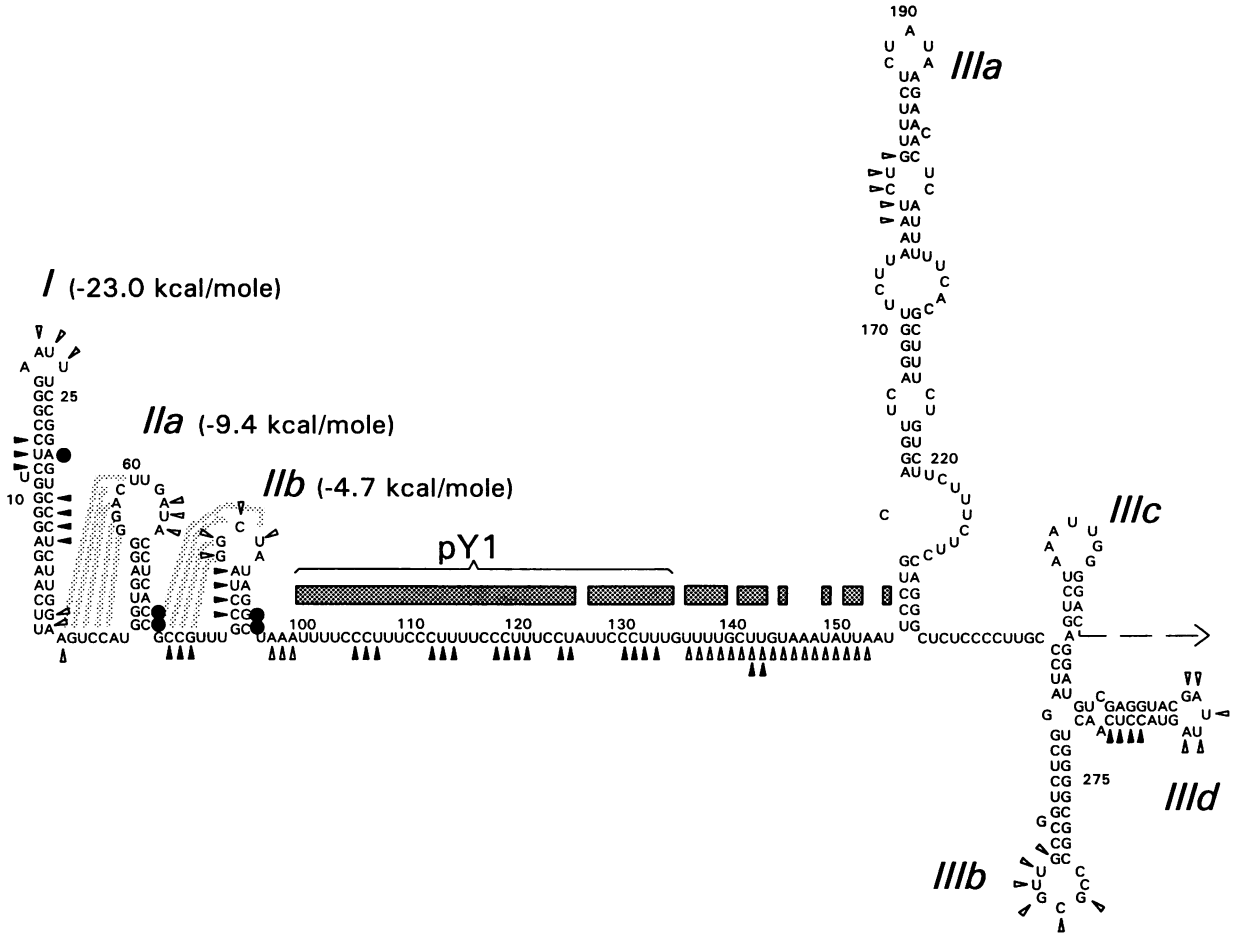

FIG. 1. Secondary structure proposed for domains I, II, and III of wild-type HM175 5'NTR RNA (3), showing sites of cleavage by single-strand-specific (T_1, T_2, and S1) nucleases (open arrowheads) and cobra venom RNase V1 (solid arrowheads). Strong primer extension stops are marked by large dots. The thermodynamic stability of stem-loops I, IIa, and IIb was calculated by the use of the RNAFOLD program (PC/Gene; Intelligenetics), adopted from Jacobson et al. (15), and does not include consideration of possible pseudoknot interactions. Pyrimidine nucleotides within the extended domain separating stem-loops IIb and IIIa (nt 95 to 154) are marked with a shaded bar.

repeats of the sequence motif (U)UUCC(C). Curiously, this motif closely resembles the core sequence of the box A motif of Pilipenko et al. (24), which is present in a conserved location in all picornaviruses, about 20 to 25 nt upstream of the initiator AUG, and which may play an important role in internal initiation of translation.

Previous modeling of the secondary structure of the 5'NTR of HM175 virus predicted that the pY1 domain and the immediately adjacent sequence from nt 139 to nt 154 were likely to be single stranded (3). Here, we present the results of RNase mapping of the secondary structure of this region of the 5'NTR and describe a series of mutant viruses with large deletions involving the pY1 domain. We show that the pY1 domain forms an ordered structural element downstream of the putative 5' pseudoknots of HAV but that this ordered structure is not required for efficient replication in cultured cells as long as the sequence between nt 140 and nt 144 is present. In contrast, an extended single-stranded region immediately downstream of the pY1 domain, which includes nt 140 to nt 144, is required for efficient replication of the virus at physiologic temperatures.

MATERIALS AND METHODS

Cells. HAV was propagated in continuous African green monkey kidney (BS-C-1) or fetal rhesus kidney (FRhK-4) cells as previously described (2).

HAV cDNA plasmids. Deletion mutations were constructed within an infectious, full-length cDNA clone of the HM175 strain of HAV (Fig. 3). The parental clone was a chimeric infectious cDNA, pG7/18fP2, which was constructed by replacing the small *Sac*I-*Eco*RI fragment of pG3/HAV7 (8, 10) (HM175/P35 virus sequence) with the corresponding cDNA fragment from a rapidly replicating, cytolytic variant (HM175/18f virus) (21), essentially replacing the P2 region of HM175/P35 with that of HM175/18f virus (28). Transfections with pG7/18fP2 RNA give rise to visible, macroscopic replication foci in radioimmunofocus assays (20) within 7 to 10 days, while transfections with pG3/HAV7 RNA generally require 14 to 21 days. Because the 5'NTR of pG7/18fP2 is derived from HM175/P35 virus (7), we refer to this plasmid as pP35-pY1 in this communication. Compared with the wild-type sequence, pP35-pY1 contains a 4-nt deletion (nt 131 to 134) and a single point mutation (nt 124, U to C) within the pY1 domain (7). For

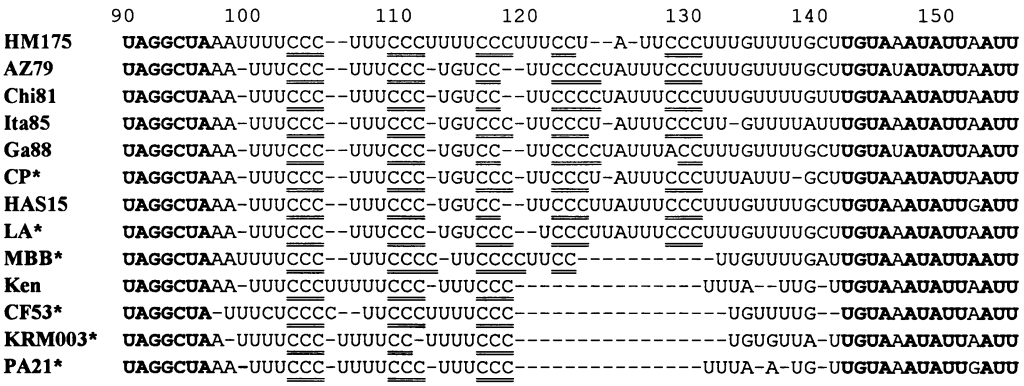

FIG. 2. Alignment of 13 human hepatovirus strains between nt 90 and nt 155 (HM175/wt sequence numbering). Strains marked with asterisks were sequenced after passage in cell culture, while others were sequenced directly from primate materials. Nucleotides flanking the region of interest which are conserved among all strains are shown in boldface type. Cytidylic acid residues within the (U)UUCC(C) motifs are indicated by a double underline. The precise origin of PA21 virus is obscure. The virus was isolated from a naturally infected captive owl monkey, but viruses with very similar nucleotide sequences have been recovered from humans (18). The sequence of Ken virus was determined from virus which had been passaged once in chimpanzees. Sequences of AZ79, Chi81, Ita85, Ga88, and Ken were provided by B. Robertson, Centers for Disease Control and Prevention, Atlanta, Ga. The sequence from strain CP was determined during the course of this work. For other sequences, see reference 3.

consistency, all nucleotide numbering is according to that of the wild-type HM175 virus sequence (9). Except where noted, manipulations of the pY1 domain were carried out in pB1.O, which contains a cDNA copy of the first 2,024 bases of the HM175/P16 (4, 17) (rather than HM175/P35) virus sequence. The pY1 domain of HM175/P16 is identical to that of the wild-type virus. Outside of the pY1 domain, the sequences of the P16 and P35 variants of HM175 differ at only a single base position in the region manipulated during mutagenesis (nt 25 to 632 [described below]). We have shown previously that these two 5′NTR sequences are functionally identical with respect to their ability to support viral replication in cultured cells (10).

Several different mutagenesis strategies were employed in constructing the deletion mutants shown in Fig. 3. The initial strategy involved construction of a subclone with unique restriction sites flanking the pY1 domain. Mutagenic oligonucleotide primers (TTTGCCTAGGCTATAGGCTCCATT [positive sense]) and (TGAACCTGCAGGAACCAATATTTA [negative sense]) were used to amplify the region between bases 78 and 168 of pB1.0 by PCR and to create *Nla*IV sites immediately downstream of the second predicted pseudoknot of domain II (stem-loop IIb [nt 95]) and immediately upstream of the first predicted stem-loop of domain III (IIIa [nt 154]) (Fig. 1) (3). The resulting 90-base PCR product containing the *Nla*IV sites was gel purified and used as the negative-strand primer in a second PCR, in which the positive-strand primer began at the −7 position relative to the HAV sequence and

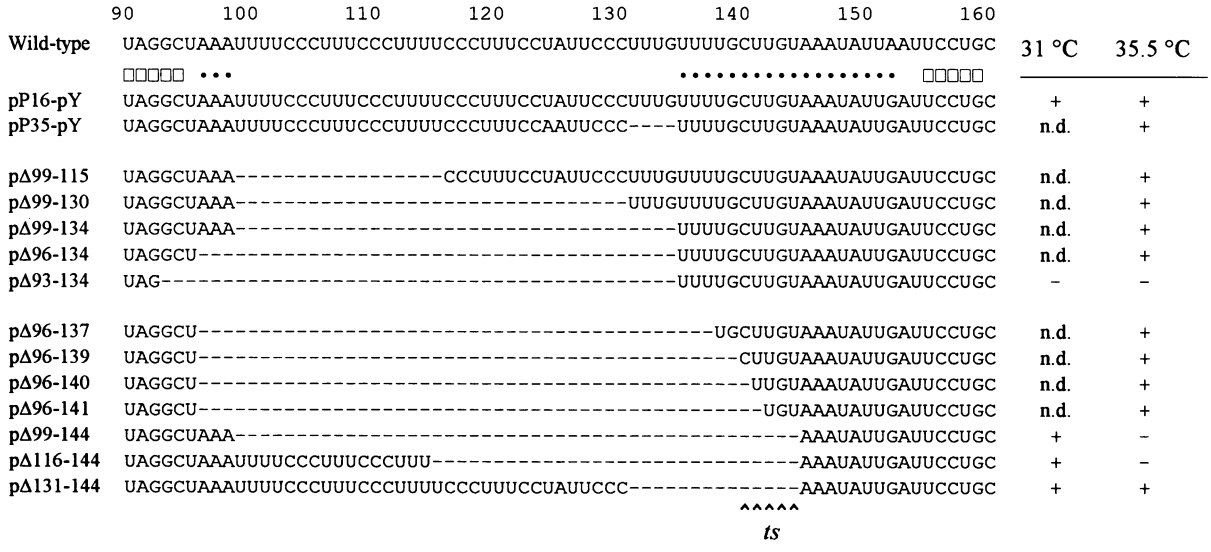

FIG. 3. pY1 deletion mutations constructed within a full-length cDNA clone of the HM175 virus. The wild-type virus sequence is shown at the top, with mutant plasmids listed at the left. Boxes represent nucleotides predicted to be involved in base-pairing interactions in stem-loops IIb (nt 90 to 94) and IIIa (nt 155 to 159); dots represent positions cleaved by single-strand-specific RNases (see Fig. 1). Direct transfection results at 31 and 37°C are shown at the right. +, replication foci demonstrated; −, no replication foci demonstrated. n.d., not determined. nt 140 to 144, which are deleted in *ts* viruses, are indicated at the bottom.

included the *Hin*dIII site at which the HAV insert is cloned in the vector. The 0.17-kb product of the second PCR was digested with *Hin*dIII and *Pst*I and then ligated with a *Pst*I-*Bam*HI fragment of pB1.0 (nt 162 to 632) into the *Hin*dIII and *Bam*HI sites of pGEM3zf(−) (Promega) to create pG3zNla. This clone contains the first 632 bases of the HM175/P16 sequence with new *Nla*IV sites at nt 95 and 154. Several clones with specific mutations within the pY1 domain were constructed by ligation of blunt-ended inserts into pG3zNla after digestion with *Nla*IV and removal of the region spanning nt 95 to 154. The three base changes which created the new *Nla*IV sites in PG3zNla were at positions 96, 97, and 153 and were thus removed prior to the ligations.

A mutant insert containing a 46-base deletion between nt 99 and nt 144 was created by annealing the two complementary oligonucleotides (TAAAAAATATTGAT [positive sense]) and (ATCAATATTTTTTA [negative sense]) and ligating the duplex into pG3zNla. The resulting subclone, containing the correct HAV sequence (HM175/P16) from 0 to 632 except for the deletion, was used to create a full-length cDNA clone, pΔ99-144 (deletion spanning nt 99 to 144) (Fig. 3), by ligating the 0.61-kb *Bsp*EI-*Bam*HI fragment (HAV sequence between base 25 and base 632) with the 9.7-kb fragment of pP35-pY1 resulting from *Bsp*EI and partial *Bam*HI digestion. As a control for these manipulations, an insert which contained the sequence of HM175/p16 virus spanning nt 96 to 155 (HM175/P16 numbering) was created with pB1.0 as the template in a PCR. This sequence was similarly introduced into pP35-pY1 to create pP16-pY1, which contains the HM175/P16 (or HM175/wt) sequence within the pY1 domain.

PCR mutagenesis was subsequently used to create a series of full-length cDNA clones with progressive deletions from the 5′ or 3′ end of the pyrimidine-rich tract. Fifty- to 60-base-long negative-sense primers containing the *Pst*I site at nt 162 were used to add back either 14 or 17 bases of the deleted pyrimidine-rich sequence to the PCR template, pΔ99-144, which lacked the entire pY1 domain. The positive-sense primer in each of these reactions spanned the *Bsp*EI site at nt 25. The resulting PCR products were digested with *Bsp*EI and *Pst*I and ligated into the unique *Bsp*EI-*Pst*I site of a subclone containing the 0.63-kb *Hin*dIII-*Bam*HI fragment of HAV (HM175/P16 sequence). Finally, a 0.61-kb product derived by digestion of this intermediate subclone with *Bsp*EI-*Bam*HI was ligated with the 9.7-kb *Bsp*EI-*Bam*HI fragment of pP35-pY1, as described above. Clones obtained in this manner included pΔ99-130 and pΔ116-144 (Fig. 3). A similar strategy, with pΔ99-130 and pΔ116-144 as templates for PCR mutagenesis, was taken to add back or delete additional nucleotides, creating pΔ99-115, pΔ99-134, and pΔ131-144. Double-stranded DNA sequencing confirmed the fidelity of PCR-amplified segments and the mutations present in individual cDNA clones.

Additional full-length mutant clones (pΔ96-134, pΔ93-134, pΔ96-137, pΔ96-139, pΔ96-140, and pΔ96-141) (Fig. 3) were created by heteroduplex site-directed mutagenesis (14), with pΔ99-134, pΔ96-134, or pΔ96-137 as the template, without construction of the intermediate subclone. Template sequence between the *Bsp*EI site (nt 25) and the *Hpa*I site (nt 353) was made single stranded in heteroduplexes formed by DNA which had been digested with *Bgl*I (first strand) or *Bsp*EI-*Hpa*I (second strand). A mutagenic oligonucleotide primer was annealed to this region, the single-stranded regions of the heteroduplexes were filled in by the Klenow fragment of DNA polymerase I, and the ends were ligated by T4 DNA ligase. All cDNA clones made by heteroduplex site-directed mutagenesis were sequenced between the *Bsp*EI and *Hpa*I sites.

Physical mapping of RNA secondary structure. RNAs representing the first 1 kb of the HAV genome were synthesized as runoff transcripts from DNA clones linearized at the *Xmn*I site (nt 980) or the *Nde*I site (nt 1108). Reaction products were digested with DNase, extracted with phenol-chloroform, and ethanol precipitated. The RNA transcripts were heated to 65°C for 3 min and allowed to cool slowly to 4°C in the presence of 10 mM $MgCl_2$–10 mM Tris (pH 7.6 or lower where indicated). Enzymatic modification of 3 μg of RNA by RNase T_1 (Pharmacia), RNase T_2 (BRL), RNase S1 (Pharmacia), or RNase V1 (Pharmacia) was carried out at room temperature in the presence of 20 μg of carrier tRNA and 10 mM $MgCl_2$–10 mM Tris (and 1 mM $ZnSO_4$ for S1 nuclease) at pH 7.6 (except where noted) in a total volume of 40 μl for 10 min. Optimal RNase concentrations were determined empirically for each batch of RNA. Reactions were stopped by the addition of excess tRNA. The modified RNA (including mock-digested RNA not subjected to nucleases) was ethanol precipitated and analyzed by primer extension with a ^{32}P-labelled negative-strand primer and 3 U of avian myeloblastosis virus reverse transcriptase (Life Sciences) at 42°C (unless otherwise noted) for 30 min (3). The primers used in these reactions included A-75 (GCCTATAGCCTAGGCAAACG), A-170 (AGAGAA ACAGATTTAAGAAC), A-241 (GCCAGAGCCTAGGGC AAGGG), and A-324 (GTGACGTTCCAAACATCTGT). Reaction products were separated on a 6% polyacrylamide gel in parallel with dideoxy sequencing reactions with unmodified RNA.

RNA transcription and transfection. Transcription reactions with SP6 RNA polymerase (Promega) were carried out in 20-μl reaction volumes, with 1.25 mM ribonucleoside triphosphates and 1.5 μg of *Hae*II-digested DNA for 90 min at 37°C. Immediately upon termination of the reaction, 18 μl of the reaction mix was mixed with 30 μl (30 μg) of Lipofectin (Bethesda Research Laboratories) diluted to 100 μl according to the manufacturer's directions and used to transfect one 60-mm petri dish culture of BS-C-1 or FRhK-4 cells. Visual inspection of transcription products in 0.1% sodium dodecyl sulfate (SDS) agarose gels indicated that the quantity of full-length 7.5-kb RNA was approximately the same in each transfection. However, in one transfection, RNA products were labelled with trace amounts of ^{32}P, and the resulting 7.5-kb bands were excised from the gel and counted with a scintillation counter. The amounts of radioactivity in the 7.5-kb bands from different transcription reactions differed by less than 20% (results not shown), confirming the validity of the visual quantitation.

For transfections, cells were washed twice with serum-free medium and fed with 2.5 ml of serum-free medium, and the RNA-Lipofectin mixture was added dropwise. After an overnight incubation, 5 ml of medium containing 10% fetal bovine serum was added to each culture. Except where noted, transfections were carried out as direct transfection and radioimmunofocus assays (10, 20). Thus, 24 h after the addition of serum-containing medium, the cells were overlaid with agarose. The cultures were incubated for 7 to 9 days at 31 to 32, 35.5, or 37°C and processed for detection of radioimmunofoci as described previously (20).

Where indicated, virus stocks were rescued from transfected FRhK-4 (or BS-C-1) cells maintained without agarose overlays. At harvest, cells were scraped into 4 ml of medium and subjected to three freeze-thaw cycles followed by brief sonication. Cellular debris was removed by low-speed centrifugation followed by chloroform extraction, and first-passage virus stocks were stored at −70°C. Higher-titer (second-passage) master seed stocks were prepared by inoculating 900-cm^2 roller

bottle cultures of confluent FRhK-4 cells with first-passage virus and harvesting as described above after 7 to 9 days of incubation at 35.5°C (or 31°C in the case of temperature-sensitive [*ts*] mutants). Working virus (third-passage) stocks were recovered by similar passage of the master seed stock in BS-C-1 cells. Virus titers are reported as radioimmunofocus-forming units of virus (rfu) per milliliter (20).

RNA sequencing. To confirm the presence of mutations in rescued viruses, the genomic RNA of working virus stocks was sequenced in the region of the pY1 domain after reverse transcription and amplification of cDNA (nt 31 to 317) by an antigen-capture-PCR method (18). The PCR product was gel purified and used as a template in cycle sequencing reactions with Δ*Taq* DNA polymerase (U.S. Biochemical Corp.). A negative-strand sequencing primer, SLA-229 (GGGGAGAGC CCTGG), was used in these reactions. The same strategy was used to sequence HAV CP.

One-step growth curve analysis of rescued virus. Approximately 2×10^5 BSC-1 or FRhK-4 cells in individual, replicate wells of a 24-well culture plate were inoculated at a high multiplicity of infection (range, 2 to 5). At specified time points, supernatant fluids were removed from the cultures. The cells were washed twice and lysed by the addition of 1 ml of 0.1% SDS as described previously (10). The viral titer of supernatant fluids or cell lysates was subsequently determined by radioimmunofocus assays carried out in BS-C-1 cells at 35.5°C (or 31°C for *ts* mutants).

Thermostability assay. Normal and *ts* virus stocks were diluted to 6.8 $\log_{10}$ rfu/ml in cell culture medium containing 3% fetal bovine serum, divided into four aliquots, and placed at 0°C. Individual aliquots of each virus stock were heated to 50, 55, or 60°C for 10 min in an automatic thermal cycler. The residual infectious virus titer was determined by radioimmunofocus assay of BS-C-1 cells at 31°C.

RESULTS

Secondary structure of the 5′ 300 nt of the 5′NTR of HAV. Covariant nucleotide substitutions within the 5′NTRs of different strains of HAV predict double-stranded helices that are conserved in the secondary structure of the RNA (3). The presence of numerous covariant substitutions provided a high level of confidence in predictions of the structure of the 3′ half of the 5′NTR, but only a single cluster of covariant substitutions (near the top of stem-loop IIIa) (Fig. 1) has been identified upstream of nt 330. Thus, previous predictions of the structure in this region of the 5′NTR (3) (Fig. 1) were based almost entirely upon thermodynamic considerations. To test the validity of these predictions, we determined the sites at which synthetic 5′NTR RNA was susceptible to cleavage by RNases which preferentially cleave single-stranded (RNase S1, RNase T_1, and RNase T_2) or double-stranded (RNase V1) RNA. The synthetic RNAs utilized in these experiments represented the 5′ 980 or 1,108 nucleotides of the HAV genome and included 10 additional nucleotides at the 5′ terminus which were derived from the vector. These experiments, the results of which are summarized in Fig. 1, generally confirmed the predicted secondary structure. Each region within the 5′ 303 nt of the 5′NTR was examined in at least two separate experiments. Representative results obtained with primer extension reactions utilizing nuclease-digested RNAs as template are shown in Fig. 4. The most prominent single-strand-specific RNAse cleavage sites were located precisely in the predicted loop regions of stem-loops I, IIa, IIb, and IIIb and at the 5′ and 3′ ends of the extended region flanking the pY1 domain (nt 96 to 98 and 135 to 152) (Fig. 1 and 4). The most prominent sites at which the double-strand-specific RNase V1 cleaved the RNA were located within the stems of stem-loops IIb (nt 81 to 84) and IIId (nt 282 to 285). Other V1 cleavage sites were at nt 74 to 76, in a region between stem-loops IIa and IIb which would be base paired in the second predicted pseudoknot (Fig. 1).

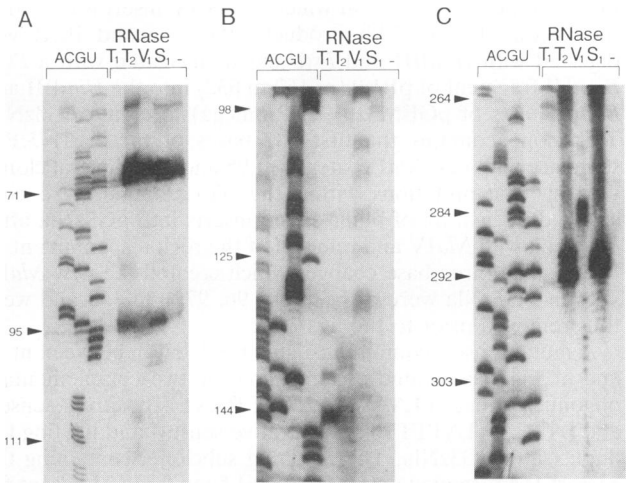

FIG. 4. Analysis of RNA secondary structure by primer extension of synthetic RNA templates which have been cleaved by single-strand-specific RNases (T_1, T_2, S1) or RNase V1. −, control lanes showing patterns with undigested RNA. Shown is the nuclease cleavage pattern for the region spanning nt 60 to 115 (A), nt 95 to 150 (B), and nt 263 to 310 (C). Lanes containing parallel sequencing ladders are indicated by ACGU. Nucleotide positions are indicated at the left. Strong nonspecific primer extension stops are located at nt 71 and 95 (A).

Surprisingly, RNase V1 cleaved the RNA at multiple sites within the pY1 domain, despite previous predictions that this region should be single stranded. These V1 cleavage sites centered on five groups of cytidylic acids that occur as part of the repetitive (U)UUCC(C) motifs (Fig. 1 and 4B), but V1 cleavage also occurred at uridylic acids located just downstream of the pY1 domain (nt 141 and 142). Significantly, no single-strand-specific enzymes cleaved the RNA within the region containing the five repetitive (U)UUCC(C) motifs (nt 99 to 130), although relatively strong single-strand cleavage sites flanked this domain. These results indicate that the pY1 domain does not exist as a randomly ordered single-stranded RNA segment but that it possesses an ordered structure. The V1 cleavages in this domain may reflect helical stacking of the RNA or possibly noncanonical hemiprotonated C-C base pairing (13) (see Discussion). Since hemiprotonated C-C base pairing is more likely to occur at acidic pH, we carried out V1 digestions over a pH range of between 7.6 and 6.0. There was no enhancement of V1 cleavage at low pH, as might be expected if C-C base pairing were occurring (data not shown). Parallel analysis of a different region of the 5′NTR confirmed that the enzyme was fully active at pH 6.0.

These experiments also provided indirect evidence for the existence of the two pseudoknots predicted to involve stem-loops IIa and IIb (Fig. 1). Strong stops for reverse transcriptase were found to occur exactly at the 3′ end of these predicted stem-loop structures (Fig. 4A). A similar strong stop was not present at the 3′ end of the 5′-terminal hairpin (stem-loop I), although a much weaker stop was sometimes observed within a G-C-rich region of this stem-loop (nt 26 to 28 [Fig. 1]). Although it is possible that the helical stems of stem-loops IIa

and IIb are sufficiently stable to inhibit the progression of reverse transcriptase, the fact that a similar strong stop was not observed at the 3′ end of stem-loop I, which is longer, more G-C rich, and predicted to have a much lower level of free energy (Fig. 1) (15), suggests that stem-loops IIa and IIb are further stabilized by their involvement in pseudoknots.

Deletion mutagenesis of the pY1 domain. Although the sequence within the pY1 domain is more variable than that in any other region of the 5′NTR (3), all human hepatovirus strains studied thus far contain a pyrimidine-rich sequence in this region which is 21 to 40 nt in length (Fig. 2). Each of these virus strains also preserves the repetitive (U)UUCC(C) motif, although the number of these motifs varies from strain to strain. To determine whether deletion mutations within and flanking the pY1 tract would impair replication, we constructed a full-length cDNA clone with a large deletion (pΔ99-144) in this domain. This deletion mutant was subsequently used for construction of additional mutants with smaller deletions (Fig. 3) (see Materials and Methods). Each of the deletion mutations was confirmed by double-stranded DNA sequencing prior to RNA transcription and transfection into permissive BS-C-1 or FRhK-4 cells. Results of transfections at 35.5 or 31°C are summarized in Fig. 3.

In direct transfection-radioimmunofocus assays carried out at 35.5°C, transfection of RNA derived from pP16-pY1, which contains the wild-type HM175 sequence in the pY1 domain, generated viral replication foci which were identical in size to those derived from RNA transcribed from the parental construct pP35-pY1 (data not shown). However, multiple transfections with pΔ99-144 RNA at standard temperature conditions of 35.5°C, in either FRhK-4 or BS-C-1 cells and including two blind passages of transfected cell harvests, never resulted in recovery of viable virus (Fig. 3). pΔ99-144 DNA was sequenced completely within the manipulated region (nt 25 to 632). There were no changes from the parental sequence other than the expected 46-nt deletion. To determine whether a lethal mutation may have occurred elsewhere in the genome, the *Bsp*EI-*Bam*HI fragment (nt 25 to 632) from pΔ99-144 was replaced with the corresponding fragment from the viable mutant pP16-pY1. As expected, RNA from the resulting clone generated replication foci that were identical in size to those of pP16-pY1. Thus, deletion of an extended sequence between stem-loops IIb and IIIa (Δ99-144 [Fig. 3]) resulted in the absence of successful RNA transfection at physiologic temperature.

RNA derived from cDNA clones with smaller deletions in the pY1 domain proved to be infectious under these conditions (Fig. 3). However, two different replication phenotypes were observed among the rescued viruses (Fig. 5 and 6). Viruses rescued from pΔ99-115, pΔ99-130, pΔ99-134, pΔ96-134, pΔ96-137, and pΔ96-139 produced replication foci which were similar in size to those of pP16-pY1. Thus, a 44-nt-long deletion mutation which included the entire pY1 domain (Δ96-139) resulted in no apparent impairment of virus replication. In contrast, virus rescued from pΔ131-144 produced very small replication foci in radioimmunofocus assays carried out at 37°C (Fig. 5). The small replication focus size observed with this virus prompted an examination of its temperature sensitivity. Parallel titrations of Δ131-144 virus in BS-C-1 cells at 31 and 37°C demonstrated a difference of 1.8 $\log_{10}$ rfu/ml in the titer of the working virus stock determined in radioimmunofocus assays carried out at these two temperatures (*ts* index), confirming that Δ131-144 virus had a *ts* replication phenotype (Fig. 6 and Table 1). In contrast, the *ts* index of P16-pY1 virus was 0.35 ± 0.08 $\log_{10}$ rfu/ml in multiple assays.

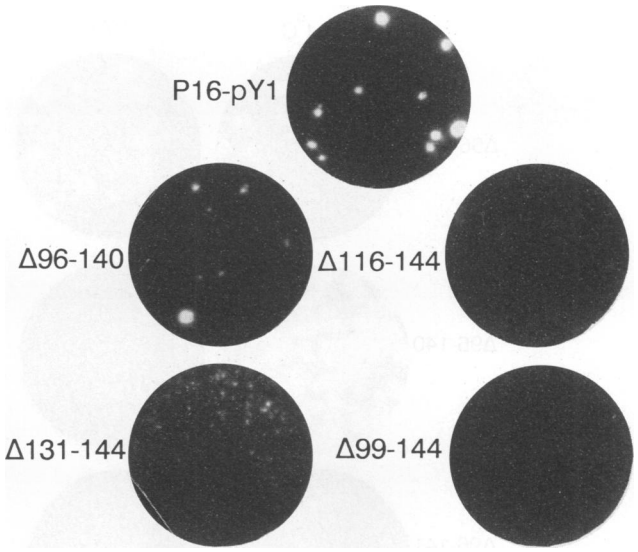

FIG. 5. Radioimmunofocus assay of virus replication at 37°C. BS-C-1 cells were infected for 9 days at 37°C with the indicated virus strains containing deletions within the pY1 region. (Negative autoradiograph image is shown.)

Consistent with these results, replication foci of Δ131-144 virus were nearly as large as those of P16-pY1 virus at 31°C (Fig. 6).

***ts* phenotypes of viruses with pY1 deletions extending to nt 140 to 144.** Recognition of the *ts* phenotype of Δ131-144 virus led us to reevaluate the infectivity of RNA transcribed from pΔ99-144 and pΔ116-144, both of which failed to generate infectious virus in transfections of FRhK-4 or BS-C-1 cells at 35.5°C (Fig. 3). Repeat RNA transfections of FRhK-4 cells at 31°C resulted in the rescue of viruses with marked *ts* phenotypes (Fig. 6). The *ts* index of Δ99-144 virus was 3.6 $\log_{10}$ rfu/ml, while that of Δ116-144 virus was 1.9 $\log_{10}$ rfu/ml (Table 1). Because the *ts* indices of the Δ96-137 and Δ96-139 viruses were 0.29 ± 0.04 and 0.40 $\log_{10}$ rfu/ml, respectively, similar to that of the parent P16-pY1 virus (Table 1), these results suggested that the 3′ extension of the deletion to include nt 140 to 144 was responsible for the *ts* replication phenotype. Interestingly, although deletion of the region spanning nt 99 to 130 (Δ99-130 and Δ99-134 viruses [Table 1]) had no significant impact on virus replication at 37°C, the deletion of this region in association with the deletion of nt 131 to 144 resulted in significant enhancement of the *ts* phenotype (compare the *ts* indices of the Δ99-144 and Δ131-144 viruses, 3.6 versus 1.8 $\log_{10}$ rfu/ml, respectively, [Table 1]). Because the *ts* index of the Δ116-144 virus was only 1.9, this enhancement of the *ts* phenotype was due primarily to deletion of the highly conserved first 2.5 (U)UUCC(C) motifs located between nt 99 and 115.

In order to define more precisely the nucleotide deletions responsible for the *ts* phenotype, two additional mutant cDNA clones were constructed, pΔ96-140 and pΔ96-141. RNA transfections at 35.5°C produced viruses with moderate *ts* phenotypes (Fig. 6). The *ts* index of Δ96-140 virus was 0.73 ± 0.17 $\log_{10}$ rfu/ml, greater than that of the parent virus P16-pY1 (0.35 ± 0.08 $\log_{10}$ rfu/ml) (Table 1). The *ts* index of Δ96-141 virus was >1.4 $\log_{10}$ rfu/ml (1.5, >1.12, and >1.5 $\log_{10}$ rfu/ml in three separate experiments). Thus, progressively greater *ts* indices were observed with viruses in which the pY1 deletion mutations extended in a 3′ direction into the sequence span-

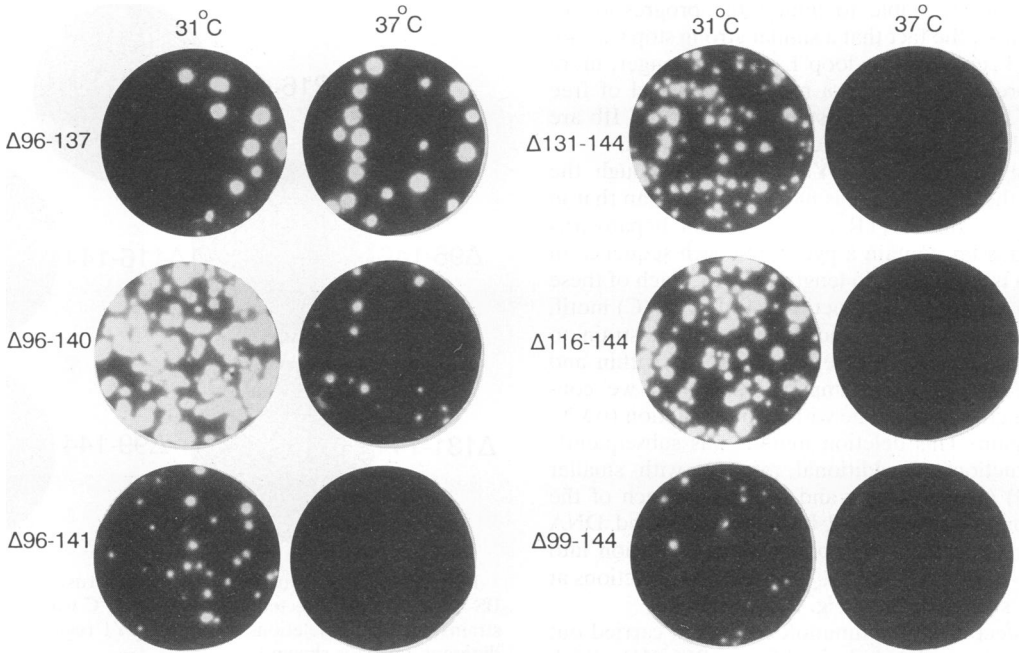

FIG. 6. Radioimmunofocus assay of virus replication at 31 or 37°C. Replicate dishes containing BS-C-1 cell monolayers were infected with identical inocula of the indicated virus strains and maintained for 9 days at either 31 or 37°C before processing for detection of radioimmunofoci. (Negative autoradiograph image is shown.)

ning nt 140 to 144 (GUUGU). However, we do not yet know whether deletion of this sequence alone confers the *ts* phenotype. Although these *ts* viruses replicated much more efficiently at the permissive temperature, the replication foci of viruses with very large deletions (Δ96-141 and Δ99-144) were smaller than those of non-*ts* viruses (e.g., Δ96-137) at 31°C (Fig. 6).

TABLE 1. Temperature sensitivity of 5′NTR deletion mutants

Virus	Radioimmunofocus size at[a]:		*ts* index[b]	Confirmed mutation[c]
	31°C	37°C		
P16-pY1	+++	+++	0.35 ± 0.08	Yes
P35-pY1	+++	+++	0.22	Yes
Δ99-115	+++	+++	0.11	Yes
Δ99-130	+++	+++	0.54	Yes
Δ99-134	+++	+++	0.21	Yes
Δ96-134	+++	+++	ND[d]	Yes
Δ96-137	+++	+++	0.29 ± 0.04	Yes
Δ96-139	+++	+++	0.40	ND
Δ96-140	++(+)	+	0.73 ± 0.17	ND
Δ96-141	++(+)	+	>1.40	Yes
Δ99-144	++	(+)	3.60	Yes
Δ116-144	++(+)	(+)	1.90	Yes
Δ131-144	++(+)	+	1.80	Yes

[a] The relative sizes of replication foci were scored subjectively. +++, equivalent to parental P16-pY1 virus; ++(+), occasionally equivalent to P16-pY1 but tending to be smaller; ++, almost always smaller than P16-pY1; +, small but always apparent foci; (+), tiny foci not always apparent in radioimmunofocus assays.

[b] *ts* index, $\log_{10}$ (titer at 31°C) − $\log_{10}$ (titer at 37°C) in radioimmunofocus assays carried out with BS-C-1 cells (± standard error when three or more assays were carried out). The Δ96-139 result is a mean of two assays, and the Δ96-141 result is a mean of three assays (see Results).

[c] Mutation confirmed by RNA sequencing of rescued virus.

[d] ND, not done.

Double-stranded DNA sequencing of the cDNA region (nt 25 to 632) manipulated during mutagenesis of two of the *ts* cDNA clones (pΔ131-144 and pΔ116-144) documented only the expected deletion mutations. Replacement of this segment in the non-*ts* pP16-pY1 clone with the corresponding segment from pΔ131-144 conferred the *ts* phenotype on the product virus, confirming that the reduced replication capacity at 37°C was due to the engineered deletion and not to an adventitious mutation elsewhere in the genome. Equally important, the expected deletions were confirmed in the RNA sequence of each of the rescued viruses (except Δ96-139 and Δ96-140, which were not sequenced) by antigen-capture-PCR of virus, followed by double-stranded DNA sequencing of the amplified product (Table 1). In no case was there reason to suspect that any of the rescued virus stocks had developed revertant or pseudorevertant mutations to compensate for the engineered deletions, since replication foci were numerous and similar in size on primary passage in direct transfection and radioimmunofocus assays.

The phenotype of individual mutants was the same after successful transfection of either BS-C-1 or FRhK-4 cells. BS-C-1 cells were consistently more difficult to transfect, but the replication foci of each of the rescued viruses were larger in BS-C-1 cells than in parallel transfections carried out with FRhK-4 cells (data not shown). This observation is consistent with the fact that each of these viruses contains cell-culture adaptation mutations at nt 152 and 203 to 204 which have been shown to promote replication of the virus in BS-C-1 cells but not in FRhK-4 cells (10).

The phenotypes of the rescued viruses remained stable for up to four passages as judged by the size of replication foci in radioimmunofocus assays. Further evidence for the stability of the *ts* phenotype was provided by experiments in which BS-C-1 cells infected with *ts* variants (Δ99-144 and Δ96-141 virus) were maintained for up to 3 weeks at the nonpermissive tempera-

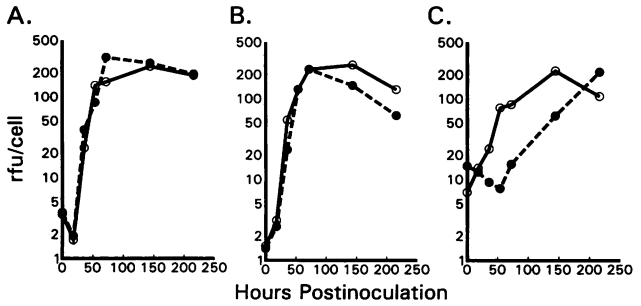

FIG. 7. Intracellular virus accumulation under one-step growth conditions at 31 or 37°C. (A) P16-pY1 virus. (B) Δ96-137 virus. (C) Δ131-144 virus. BS-C-1 cells were infected with a virus inoculum calculated to provide a multiplicity of infection of approximately three infectious particles per cell and then incubated at either 31°C (○) or 37°C (●). At the indicated time points, monolayers were washed and lysed by the addition of 0.1% SDS. Virus titers in lysates were determined by radioimmunofocus assay of BS-C-1 cells at 31°C.

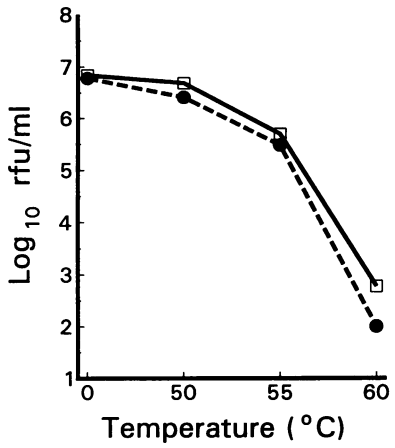

FIG. 8. Thermostability of the P16-pY1 (□) and *ts* Δ131-144 (●) viruses. Virus stocks were incubated at the indicated temperatures for 10 min, and the surviving virus titer was determined by radioimmunofocus assay of BS-C-1 cells at 31°C.

ture (37°C) after an initial 24-h incubation at the permissive temperature (31°C). Virus harvests prepared from these cells were subsequently tested with radioimmunofocus assays at the nonpermissive temperature in order to detect large-focus revertants. No such revertants were isolated (data not shown).

Analysis of *ts* virus replication under one-step growth conditions. Although radioimmunofocus size is an accurate measure of the replication efficiency of HAV in cultured cells (10), BS-C-1 and FRhK-4 cells were infected under one-step growth conditions in order to quantitate better the differences in the kinetics of replication of different deletion mutants. At the permissive temperature (31°C) in BS-C-1 cells, the replication of Δ131-144 virus (*ts* index, 1.8) was somewhat delayed compared with replication of the parental P16-pY1 virus or the large deletion mutant Δ96-137 (Fig. 7). The latter two viruses demonstrated similar replication kinetics, with virus yields approaching maximum by 72 h postinoculation. In contrast, maximum yields of Δ131-144 were not reached until 144 h postinoculation. This difference in replication kinetics was reflected also in the somewhat smaller size of Δ131-144 replication foci at 31°C (Fig. 6). The higher intracellular virus titer immediately after adsorption of Δ131-144 (time 0 [Fig. 7]) likely reflects a higher multiplicity of infection in cells inoculated with the Δ131-144 virus.

At the nonpermissive temperature (37°C), replication of Δ131-144 virus was further delayed, with no increase over input virus noted until after 72 h postinoculation. Between 72 and 216 h, the increase in the titer of Δ131-144 virus paralleled that observed between 18 and 72 h at the permissive temperature (Fig. 7). In contrast, there was no difference in the growth kinetics of P16-pY1 and Δ96-137 viruses at 31 and 37°C, consistent with the low *ts* indices of these viruses (Table 1). The fact that the rate of intracellular accumulation of Δ131-144 virus between 72 and 216 h at the nonpermissive temperature paralleled the rate of accumulation between 12 and 150 h at the permissive temperature (Fig. 7C) suggests that the *ts* phenotype of Δ131-144 might be due to a *ts* step occurring relatively early in the virus replication cycle. Additional one-step growth experiments confirmed that the replication of Δ131-144 virus was significantly delayed in comparison with that of the P16-pY1 and Δ100-131 viruses at 35.5°C in both FRhK-4 and BS-C-1 cells (data not shown). In general, in these one-step growth experiments, the final virus yield obtained with the *ts* Δ131-144 virus was similar to that obtained with the non-*ts* viruses.

Contribution of P2 region mutations to the *ts* phenotype. All of the deletion mutants described above were constructed in a background which included the P2 genomic region of the rapidly replicating, cytopathic strain HM175/18f (28) (see Materials and Methods). Thus, it was possible that the *ts* phenotype of the mutants described above might be derived in part from one or more of the numerous mutations present in the P2 region (21). To address this possibility, the P2 region from the cell culture-adapted HM175/P35 variant (pHAV/7) (8) was reintroduced into the *ts* cDNA clone pΔ131-144 to produce pΔ131-144/P2P35. Virus rescued from pΔ131-144/P2P35 RNA demonstrated a *ts* phenotype similar to that of Δ131-144 virus (data not shown), indicating that the *ts* phenotype was not codependent upon the presence of HM175/18f P2 region mutations. However, as expected, this virus replicated much more slowly than Δ131-144, requiring 2 to 3 weeks for demonstration of replication foci after RNA transfection, even at the permissive temperature.

Thermostability of *ts* virus particles. We compared the thermostability of the Δ131-144 virus with that of the P16-pY1 parent in order to determine whether the reduction in titer of this *ts* strain at the nonpermissive temperature might reflect increased thermolability of virions due to altered interactions between capsid proteins and genomic RNA. The infectious titers of the P16-pY1 and Δ131-144 viruses were reduced to a similar extent after brief incubation at temperatures ranging from 50 to 60°C (Fig. 8). Thus, the *ts* phenotype of Δ131-144 virus is not related to reduced thermostability of the virus.

Deletion mutation involving stem-loop IIb. All of the deletion mutations described above were located between stem-loop structures predicted to flank the pY1 region (Fig. 1). To determine the impact of extension of these deletions in a 5′ fashion into stem-loop IIb, an additional cDNA mutant (pΔ93-134) was constructed. Compared with the viable pΔ96-134 mutant, the deletion mutation in pΔ93-134 extends in a 5′ direction by an additional 3 nt and includes the 3′-terminal 2 nt of stem-loop (pseudoknot) IIb (Fig. 1 and 3). Multiple transfections of FRhK-4 or BS-C-1 cells with RNA derived from pΔ93-134, at either 31 or 35.5°C, failed to yield infectious virus (Fig. 3). In addition, a serendipitously discovered second-site cDNA mutant derived from the viable pΔ99-134 mutant, which had an additional, random mutation involving a G-to-U sub-

stitution at nt 85, also failed to produce infectious virus after RNA transfection (data not shown). The G-to-U substitution at nt 85 would be predicted to destabilize the putative pseudoknot involving stem-loop IIb (Fig. 1). These data suggest that retention of the secondary and possibly tertiary RNA structure in this region of the 5′NTR is essential for infectivity of the virus and provide further indirect support for the proposed structural model.

DISCUSSION

Although somewhat analogous to the poly(C) tracts of cardioviruses and aphthoviruses in terms of base composition and position within the 5′NTR, the mixed UC-rich pY1 tract of the hepatoviruses is unique among picornaviruses. Among different human hepatovirus strains, there is substantial sequence heterogeneity within this region of the 5′NTR (3). However, a strikingly conserved feature of the pY1 tract of all human hepatoviruses studied thus far is the presence of three to five repeated (U)UUCC(C) motifs (Fig. 2). The function of the pY1 domain, which is located upstream of the IRES (4), is unknown. However, in UV cross-linking-label transfer experiments, a short RNA probe (nt 95 to 154) containing the pY1 domain and the adjacent downstream single-stranded region was more active than any other probe from the 5′NTR in binding polypyrimidine tract binding protein from HeLa cells as well as unidentified, ribosome-associated 30- and 39-kDa proteins present in BS-C-1 and FRhK-4 cells permissive for HAV replication (5). To gain a better understanding of the structure and function of this pyrimidine-rich tract, we engineered a series of large deletions within the pY1 domain of a full-length, infectious cDNA copy of the HM175 strain genome. These studies were substantially aided by the availability of an infectious cDNA clone containing the P2 genomic region of a rapidly replicating, cytopathic (RR/CPE+) variant of the HM175 virus, which permits recovery of virus within 7 days of transfection of BS-C-1 or FRhK-4 cells with in vitro-transcribed RNA (28).

Virus mutants with deletions in the pY1 region which were rescued from transfected cells demonstrated two distinctly different replication phenotypes. Five mutant viruses with deletions ranging from 14 to 46 nt in length and extending into the critical domain of nt 140 to 144 (Δ99-144, Δ116-144, Δ131-144, Δ96-140, and Δ96-141) were found to have a *ts* replication phenotype. If the entire sequence between nt 140 and nt 144 was removed, the resulting viruses were strongly *ts* (Δ99-144, Δ116-144, and Δ131-144). These viruses demonstrated a reduction in viral titer at the nonpermissive temperature (*ts* index) ranging from 1.8 to 3.6 $\log_{10}$ rfu/ml (Table 1). In contrast, a second group of mutant viruses with equally large deletions, up to 44 nt in length, but not involving nt 140 to 144, replicated as efficiently as the parental virus at 37 and 31°C. These data indicate that the pY1 domain (nt 99 to 138) of HM175 virus is not required for replication in cultured cells, while the flanking single-stranded domain (nt 140 to 144) is essential for efficient replication at physiological temperatures. The marked difference between the *ts* index of the Δ99-144 mutant and those of the Δ116-144 and Δ131-144 mutants (3.6 versus 1.9 and 1.8 $\log_{10}$ rfu/ml, respectively [Table 1]) demonstrates that the additional deletion of sequence elements within the pY1 domain (particularly nt 99 to 115) substantially enhances the *ts* phenotype of virus lacking nt 131 to 144. The critical *ts* domain (CUUGU, nt 140 to 144) is located at the 3′ end of the pY1 tract (Fig. 1). These nucleotides are part of a larger single-stranded segment which is accessible on the surface of the tertiary structure of the folded RNA, as evidenced by the ability of single-strand-specific RNases to cleave within the sequence spanning nt 135 to 152 (Fig. 1 and 4). Although it is apparently not involved in base-pairing interactions with other regions of the 5′NTR, this short segment, especially the trinucleotide sequence UGU (nt 142 to 144), is very well conserved among different hepatovirus strains (Fig. 2).

The function of this single-stranded segment just downstream of the pY1 domain (Fig. 1) (3) is unclear. Previous studies do not support a critical role for this segment of the HAV 5′NTR in internal initiation of translation. Translation studies with rabbit reticulocyte lysates programmed with 5′-terminally deleted monocistronic HAV transcripts (3) or bicistronic transcripts in which 5′NTR sequences were present in the intercistronic space (4) suggest that the IRES is located downstream of nt 152, entirely 3′ of the pY1 tract and the adjacent single-stranded domain. More recent studies carried out in vivo with permissive monkey kidney cells have shown that removal of the first 161 nt of the 5′NTR does not impair and may even enhance by severalfold the translation of uncapped, monocistronic RNA transcripts containing a reporter gene fused to the 5′NTR of HAV (27). These data indicate that the pY1 tract and the adjacent single-stranded domains are not required for translation initiation in vitro or in vivo. Thus, the observed *ts* replication phenotype is more likely to be related to impaired RNA replication or possibly to defects in assembly and packaging. However, it is possible that deletions in the critical *ts* domain between nt 140 and nt 144 may affect folding of downstream RNA and thus have an effect on translation. Further studies are required to distinguish between these possibilities.

Large pY1 tract deletions which did not involve the critical nt 140 to 144 domain had no apparent effect on the replication of virus in FRhK-4 or BS-C-1 cell cultures maintained at physiologic temperatures (Table 1). That this might be the case was suggested in part by the presence of smaller pY1 deletions in the sequences of other hepatovirus strains (Fig. 2). The sequence of several of these strains, MBB (23), CF53, and PA21 (3) was obtained from RNA isolated from cell culture-adapted variants, and thus these deletions may have occurred during adaptation and passage in cultured cells. As shown in Fig. 3, a 4-nt deletion (nt 131 to 134) is known to have occurred in this domain during adaptation and passage of the HM175 strain in cell culture (7).

The RNA sequence in the dispensable pY1 domain appears to possess an ordered structure. Nuclease cleavage analysis of synthetic RNA indicated that the AAA triplet at nt 96 to 98 is located in a single-stranded region and is accessible to enzymatic cleavage, as is the single-stranded sequence from nt 135 to 152 (Fig. 1 and 4). However, there were no clear single-strand-specific RNase cleavage sites in the intervening region spanning nt 99 to 134. Instead, the phosphodiester backbone was generally subject to RNase V1 cleavage at the 3′ side of the cytidylic acid residues within the (U)UUCC(C) motifs of the pY1 domain, indicating that the pY1 domain is accessible to nuclease attack (Fig. 1 and 4). V1 nuclease has strong substrate preference for double-stranded RNA but is known to cleave synthetic, single-stranded homopolymers which are capable of assuming a stacked helical structure (22). It is unlikely that the pY1 domain forms extensive duplexes with other regions of the viral RNA through conventional Watson-Crick base pairs, because complementary sequence is lacking elsewhere in the 5′NTR and because sequence covariance does not occur at other 5′NTR sites in those strains with variable pY1 sequences (3).

It is possible that these V1 cleavage sites are related to

single-stranded helical stacking of the RNA within the pY1 domain. A similar phenomenon may explain the V1 cleavages at nt 141 and 142, which are within a region of the RNA that is cleaved by multiple single-strand-specific RNases (Fig. 1 and 4B). Previous studies have shown that V1 nuclease cleaves RNA at any accessible position at which the sugar phosphate backbone assumes a helical conformation, whether the bases are paired or not (22). On the basis of the absence of cleavage by *Bacillus cereus* RNase, Escarmis et al. (12) suggested that the lengthy poly(C) tract of aphthoviruses possesses a helical stacked secondary structure. Alternatively, the V1 cleavage sites may be related to noncanonical base pairing involving the cytidylic acid residues of the (U)UUCC(C) motifs. Cytosines protonated at N^3 can form noncanonical base pairs with unprotonated cytosines (13). These hemiprotonated C-C base pairs are stabilized by three hydrogen bonds and can direct the formation of parallel-stranded duplexes and anti-parallel tetrads. Such interactions might be stable and biologically important at physiological pH (13). However, RNase VI digestions carried out under conditions of lower pH did not demonstrate a clear enhancement of the cleavage reaction (data not shown), as might be expected were these cleavages dependent upon the presence of hemiprotonated C-C base pairs. Whatever the basis for the ordered V1 cleavage sites within the pY1 domain, this finding has obvious relevance to the poly(C) tracts of the cardioviruses and aphthoviruses. Like the pY1 domain of HAV, the poly(C) tract of the cardioviruses (11) is not required for efficient replication in cultured cells (Fig. 6).

Although the pyrimidine-rich sequence between nt 96 and nt 139 is completely dispensable for efficient replication in cultured cells, it is unlikely that most or all of this domain would be retained by wild-type human hepatoviruses (Fig. 2) were it not required at some stage in the virus life cycle. Duke et al. (11) have shown that the length of the poly(C) tract of mengovirus determines virulence in the murine host. Mutant mengoviruses lacking this tract are able to replicate efficiently in cell culture but are stably attenuated by many orders of magnitude. In contrast, genetically engineered short poly(C) variants (C_6-C_{35}) of foot-and-mouth disease virus gave rise to longer poly(C) variants (C_{75}-C_{140}) after a single passage in cell culture, suggesting that longer poly(C) tracts favor replication in cultured cells (26). In addition, a C_2 strain of foot-and-mouth disease virus was shown to be virulent in mice, in contrast to the short poly(C) strains of mengovirus (26). Because the HAV pY1 tract is not required for replication in cell culture, the pY1-deleted HAV mutants described in this paper resemble short poly(C) mutants of mengovirus more than short poly(C) foot-and-mouth disease virus mutants. Since the poly(C) tract of mengovirus results in attenuation in the natural host, it will be of substantial interest to learn whether large pY1 deletions similarly result in attenuation of HAV in primates. Similarly, the *ts* replication phenotype conferred by the deletion of nt 140 to 144 may also be relevant to the design of better attenuated HAV vaccines. Specific mutations resulting in *ts* replication phenotypes have not been described previously for HAV, and it is tempting to speculate that novel vaccine candidates with useful attenuation phenotypes might be derived by the inclusion of such mutations in HAV variants which have undergone relatively few passages in cell culture and which otherwise remain virulent for primates.

ACKNOWLEDGMENTS

We thank Charles Hardin for stimulating discussions of the secondary structure of the pY1 domain, Betty Robertson for providing unpublished 5'NTR sequences from the AZ79, Chi81, Ita85, Ga88, and Ken hepatovirus strains (Fig. 2), Hangchun Zhang for the use of plasmid pG7/18fp2, and Paula Murphy for excellent technical assistance.

This work was supported by grants from the Public Health Service (RO1-AI32599, and T32-AI07001), the U.S. Army Medical Research and Development Command (DAMD 17-89-Z-9022), and the World Health Organization's Programme for Vaccine Development (V24/181/28).

REFERENCES

1. **Andino, R., G. E. Rieckhof, and D. Baltimore.** 1990. A functional ribonucleoprotein complex forms around the 5′ end of poliovirus RNA. Cell **63**:369–380.
2. **Binn, L. N., S. M. Lemon, R. H. Marchwicki, R. R. Redfield, N. L. Gates, and W. H. Bancroft.** 1984. Primary isolation and serial passage of hepatitis A virus strains in primate cell cultures. J. Clin. Microbiol. **20**:28–33.
3. **Brown, E. A., S. P. Day, R. W. Jansen, and S. M. Lemon.** 1991. The 5′ nontranslated region of hepatitis A virus RNA: secondary structure and elements required for translation in vitro. J. Virol. **65**:5828–5838.
4. **Brown, E. A., A. J. Zajac, and S. M. Lemon.** 1994. In vitro characterization of an internal ribosomal entry site (IRES) present within the 5′ nontranslated region of hepatitis A virus RNA: comparison with the IRES of encephalomyocarditis virus. J. Virol. **68**:1066–1074.
5. **Chang, K. H., E. A. Brown, and S. M. Lemon.** 1993. Cell type-specific proteins which interact with the 5′ nontranslated region of hepatitis A virus RNA. J. Virol. **67**:6716–6725.
6. **Clarke, B. E., A. L. Brown, K. M. Currey, S. E. Newton, D. J. Rowlands, and A. R. Carroll.** 1987. Potential secondary and tertiary structure in the genomic RNA of foot and mouth disease virus. Nucleic Acids Res. **15**:7066–7079.
7. **Cohen, J. I., B. Rosenblum, J. R. Ticehurst, R. J. Daemer, S. M. Feinstone, and R. H. Purcell.** 1987. Complete nucleotide sequence of an attenuated hepatitis A virus: comparison with wild-type virus. Proc. Natl. Acad. Sci. USA **84**:2497–2501.
8. **Cohen, J. I., J. R. Ticehurst, S. M. Feinstone, B. Rosenblum, and R. H. Purcell.** 1987. Hepatitis A virus cDNA and its RNA transcripts are infectious in cell culture. J. Virol. **61**:3035–3039.
9. **Cohen, J. I., J. R. Ticehurst, R. H. Purcell, A. Buckler-White, and B. M. Baroudy.** 1987. Complete nucleotide sequence of wild-type hepatitis A virus: comparison with different strains of hepatitis A virus and other picornaviruses. J. Virol. **61**:50–59.
10. **Day, S. P., P. Murphy, E. A. Brown, and S. M. Lemon.** 1992. Mutations within the 5′ nontranslated region of hepatitis A virus RNA which enhance replication in BS-C-1 cells. J. Virol. **66**:6533–6540.
11. **Duke, G. M., J. E. Osorio, and A. C. Palmenberg.** 1990. Attenuation of Mengo virus through genetic engineering of the 5′ noncoding poly(C) tract. Nature (London) **343**:474–476.
12. **Escarmís, C., M. Toja, M. Medina, and E. Domingo.** 1992. Modifications of the 5′ untranslated region of foot-and-mouth disease virus after prolonged persistence in cell culture. Virus Res. **26**:113–125.
13. **Gehring, K., J.-L. Leroy, and M. Gueron.** 1993. A tetrameric DNA structure with protonated cytosine-cytosine nucleotide pairs. Nature (London) **363**:561–565.
14. **Inouye, S., and M. Inouye.** 1987. Oligonucleotide-directed site-specific mutagenesis using double-stranded plasmid DNA, p. 181–206. *In* S. A. Narang (ed.), Synthesis and applications of DNA and RNA. Academic Press, Orlando, Fla.
15. **Jacobson, A. B., L. Good, J. Simonetti, and M. Zuker.** 1984. Some simple computational methods to improve the folding of large RNAs. Nucleic Acids Res. **12**:45–52.
16. **Jang, S. K., M. V. Davies, R. J. Kaufman, and E. Wimmer.** 1989. Initiation of protein synthesis by internal entry of ribosomes into the 5′ nontranslated region of encephalomyocarditis virus RNA in vivo. J. Virol. **63**:1651–1660.
17. **Jansen, R. W., J. E. Newbold, and S. M. Lemon.** 1988. Complete nucleotide sequence of a cell culture-adapted variant of hepatitis A virus: comparison with wild-type virus with restricted capacity for *in vitro* replication. Virology **163**:299–307.
18. **Jansen, R. W., G. Siegl, and S. M. Lemon.** 1990. Molecular

epidemiology of human hepatitis A virus defined by an antigen-capture polymerase chain reaction method. Proc. Natl. Acad. Sci. USA **87:**2867–2871.

19. **Kühn, R., N. Luz, and E. Beck.** 1990. Functional analysis of the internal translation initiation site of foot-and-mouth disease virus. J. Virol. **64:**4625–4631.
20. **Lemon, S. M., L. N. Binn, and R. H. Marchwicki.** 1983. Radioimmunofocus assay for quantitation of hepatitis A virus in cell cultures. J. Clin. Microbiol. **17:**834–839.
21. **Lemon, S. M., P. C. Murphy, P. A. Shields, L.-H. Ping, S. M. Feinstone, T. Cromeans, and R. W. Jansen.** 1991. Antigenic and genetic variation in cytopathic hepatitis A virus variants arising during persistent infection: evidence for genetic recombination. J. Virol. **65:**2056–2065.
22. **Lowman, H. B., and D. E. Draper.** 1986. On the recognition of helical RNA by cobra venom V1 nuclease. J. Biol. Chem. **261:** 5396–5403.
23. **Paul, A. V., H. Tada, K. von der Helm, T. Wissel, R. Kiehn, E. Wimmer, and F. Deinhardt.** 1987. The entire nucleotide sequence of the genome of human hepatitis A virus (isolate MBB). Virus Res. **8:**153–171.
24. **Pilipenko, E. V., A. P. Gmyl, S. V. Maslova, Y. V. Svitkin, A. N. Sinyakov, and V. I. Agol.** 1992. Prokaryotic-like cis elements in the cap-independent internal initiation of translation on picornavirus RNA. Cell **68:**119–131.
25. **Pleij, C. W. A.** 1990. Pseudoknots in noncoding regions of viral RNAs, p. 49–50. Proc. VIIIth Int. Congr. Virol.
26. **Rieder, E., T. Bunch, F. Brown, and P. W. Mason.** 1993. Genetically engineered foot-and-mouth disease viruses with poly(C) tracts of two nucleotides are virulent in mice. J. Virol. **67:**5139–5145.
27. **Whetter, L. E., S. P. Day, O. Elroy-Stein, E. A. Brown, and S. M. Lemon.** 1994. Low efficiency of the 5′ nontranslated region of hepatitis A virus RNA in promoting cap-independent translation in permissive monkey kidney cells. J. Virol. **68:**5253–5263.
28. **Zhang, H.-C., L.-H. Ping, and S. M. Lemon.** Unpublished data.